Eng. Sci., 2020, 11, 3-18

Engineered Science

DOI: https://dx.doi.org/10.30919/es8d0013

Ionic Liquids as "Green Solvent and/or Electrolyte" for Energy Interface

Zhe Wang,[1,2,*] Shuangding He,[3] Vincent Nguyen[2] and Kevin E. Riley[2]

Abstract

Ionic Liquids (ILs) as a class of materials that are composed of cations and anions have been attracted much attention and used in a variety of applications. Due to the negligible volatility, high chemical and thermal stability, high ionic conductivity and wide electrochemical window, ILs have been used in the electrochemical devices, electrocatalysis, extraction, electrosynthesis, gas absorption and sensors. In addition to the application in electrochemical devices, ILs have been used in energy transformation devices. Therefore, in this review, we have focused on mainly the applications of ILs in electrochemical energy storage, energy conversion and CO_2 reduction. We also discuss the current trend of computational design for ILs electrochemical system and IL-like ion conductor from nature, which could be employed in green electrochemistry applications in the future.

Received: 13 April 2020; Accepted: 9 June 2020.
Article type: Review article.

1. Introduction

Green energy is derived from natural resources such as sunshine, wind, storms, oceans, seeds, algae and geothermal energy.[1-3] These sources of energy are renewable, which means that they are naturally replenished. Fossil fuels, on the other hand, are a finite resource, taking millions of years of growth and rising as they are used. Renewable energy has a much smaller impact on the environment than fossil fuels, which contribute to climate change by producing pollutants such as greenhouse gases as byproducts.[4-6] Fossil fuels often require mining or drilling deep into the earth in ecologically sensitive locations. However, the energy available for green energy is readily available around the world, including in rural and remote areas without electricity. Advances of renewable energy technologies have lowered the cost of solar panels, wind turbines, and other green energy, allowing people to generate power instead of oil, gas, coal, and utilities.[7-9] Green energy will replace fossil fuels in all main applications, including power, water and space heating and vehicle gasoline. Investments in green energy production and advancement should thus be encouraged by governments and other authorities for green energy replacement of fossil fuels for a more environmentally sound and sustainable future.[10-12]

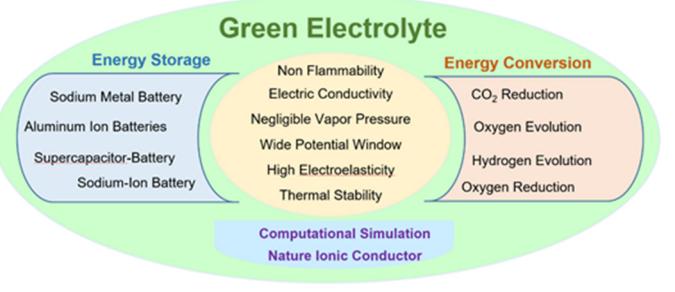

Scheme 1. The properties of ionic liquid as a green electrolyte for energy storage and conversion and future directions.

Ionic Liquids (ILs) are classified as molten salts with melting points below 100 °C, most of which are organic salts with a broad variety of designs.[12-14] These are known as the third group of solvents (and electrolytes) after water and organic solvents and are usually distinguished by unique properties such as non-volatility, strong thermal stability, and high ion conductivity.[13,15-16] ILs supports offer a better loading capacity than solid supports. Nevertheless, these properties are strongly affected by Lewis acidity/basicity of cations/anions (i.e. Coulombic interactions), spatial interactions between cations and anions, and van der Waals interactions between ions.[17] The strain of IL as an electrolyte component is very important due to its tunable characteristics, high electrochemical and thermal stability, low O_2^{-}·reactivity and low volatility and flammability.[18] Among these very

[1] *Oakland University, Rochester, USA, 48309.*
[2] *Xavier University of Louisiana, New Orleans, USA, 70002.*
[3] *Pioneer Academy Wayne, New Jersey, USA, 07470.*
[*] *E-mail: zhewang188@gmail.com, zhewang@oakland.edu (Z. Wang).*

interesting compounds, imidazole and pyrrolidinium-based electrolytes have shown promising results in lithium and sodium batteries.[19-21] In other words, with regard to the properties of ILs, it should be understood with the utmost care that the characteristics mentioned above are not always provided by all ILs, which, in turn, provide scope for the design of new task-specific ILs, such as the battery, capacitor sensor and catalytic systems.[22-26] The energy production through the IL-based systems and supercapacitor applications have been reviewed.[27-29] However, the exploration and understanding of ILs as both solvent and electrolyte for the new device systems such as Al oxygen/ion battery, supercapacitor battery, CO_2 reduction and *et.al*. are in their infancy. In this review article, recent progress in the study and use of ILs energy storage and conversion in the newly developed systems (Scheme 1), its fundamental design and the future potential of IL-like ion conductor from nature will be discussed.

2. Current Progress

2.1. Application of ILs in electrochemical energy storage

The demand for energy storage and conversion is increasing, and the battery and capacitor are becoming the main storage materials for energy.[30-33] However, the current lithium-ion battery also has a lack of lithium resources, and expensive, short-lived battery and a number of weaknesses. The introduction of sodium-ion batteries also provided an alternative to lithium-ion batteries.[34-36] The Na-S battery was designed by Ford but needed 300 °C to sustain the molten process between the two active materials, which resulted in low energy performance.[37-39] Aseveral studies have been carried out using enhanced electrochemical efficiency of EMIMFSI IL-based gel polymer electrolyte with temperature for rechargeable lithium batteries.[40-42] Rechargeable aluminum ion batteries (RABs) have attracted a lot of attention due to their high charging capacity, low cost and reduced flammability.[43-45] The special conversion mechanism of the Al battery chemistry stops cathode content from disintegrating through repetitive charging-discharge cycles, and this device effectively suppresses the IL dissolved polyiodide shuttle due to hydrogen bonding activity, resulting in a powerful rechargeable RAB method, which provides new insight into the designing system based on redox chemistry.[46-49] Here we summarized the most recent progress made by using ILs as a green electrolyte for the energy storage system.

2.1.1 IL in lithium-oxygen battery

The disadvantages of the lithium-oxygen battery hinder its applicability. Singh's group is trying to identify electrode materials with better stability and greater strength. Rechargeable lithium-ion batteries, supercapacitors, and other highly efficient energy storage devices are needed worldwide. Among the numerous electrolytes available, polymer electrolytes (PEs) are preferred over liquid electrolytes because they overcome the above-mentioned problems associated with liquid electrolytes and also offer several advantages such as the ability to form a thin film, flexibility, good electrode contact and convenience of preparation.[50] Normally, PEs are of two types: solid polymer electrolytes (SPEs) and gel polymer electrolytes (GPEs). SPEs are prepared using polar polymers (like polyvinyl acetate (PVA), polyethylene oxide (PEO), polymethylmethacrylate (PMMA), polyvinylidene fluoride (PVDF), etc.) with ionic salts (like $LiPF_6$, $LiBF_4$, $LiClO_4$ and LiTFSI, etc.). However, the room temperature conductivity of SPEs was not as good as desired for use in Lithium-ion battery (LIBs). Armand *et al*. recorded ion conductivity ~10^{-5} S cm^{-1} at 40 °C in PEO dependent SPE for LIB use.[51] As a result, many researchers have focused on increasing the performance (such as ion conductivity, electrochemical stability, etc.) of SPEs.[52]

Various approaches have been used to enhance the ionic conductivity of SPEs. One of the possible solutions is the processing of GPEs, owing to their many advantages over SPEs, such as increased mechanical durability, versatility, enhanced ion conductivity, strong interfacial interaction with electrodes, etc. Organic plasticizers such as ethylene carbonate (EC), propylene carbonate (PC), dimethyl carbonate (DMC) can be used to prepare GPEs,[53] etc. Since these organic plasticizers can improve ionic conductivity by several orders of magnitude but show poor chemical, thermal and electrochemical stability due to their volatile nature.[54] A promising approach is now being adopted to develop high-temperature sustainable GPEs for LIB applications in which organic plasticizers are replaced by room temperature ILs (RTILs). RTILs have been deemed a perfect ionic solvent owing to some unique properties such as moderate ionic conductivity (~0.01 S cm^{-1}), outstanding thermal stability (~400 °C – 500 °C), strong electrochemical stability (~4.0 V – 6.0 V), non-flammability, non-volatility, simple miscibility with organic solvents, marginal vapor pressure, and reasonable plasticization potential, which improves the amorphicity of the polymer matrix. RTILs are therefore used in a number of electrochemical applications, such as rechargeable batteries, supercapacitor, fuel cells, solar cells etc.[55-56] ILs can be classified according to electrochemical stability, ion conductivity and electrode compatibility. Among them, phosphonium-and ammonium-based ILs families demonstrated better electrochemical stability and good cyclic performance at low current rates when used in LIBs.[57] But, imidazolium-based ILs are also offering applicants for use in LIBs due to many important properties such as high thermal stability, low viscosity, high ionic conductivity, a wide electrochemical working window and good cycle performance at high current rate etc.[58-59] Thus, ILs need to be stored in SPEs that provide strong ion conductivity and reasonable electrochemical/thermal stability.[60-61] Some publications on IL-based GPEs for lithium metal polymer batteries (LMPBs) applications also have been reviewed, for example, Kim *et al*. observed that Li/$P(EO)_{10}$LiTFSI + $_{0.96}PYR_{1A}$TFSI/$LiFePO_4$ was capable of producing a discharge capacity of ~84.1 mAh

g^{-1} at a rate of 0.1 C at 25 °C.[62] and Li *et al*. reveals the electrochemical performance of the Li/$LiFePO_4$ cell using the $PRY_{14}TFSI$ IL-based gel polymer electrolyte, which received a discharge capacity of ~120.4 mAh g^{-1} at a rate of 0.1 C at room temperature.[63] Zhu *et al*. published the ionic conductivity value of pyridinium-based electrolyte ($P(EO)_{20}LiTFSI$+1.0PP13-TFSI) ~ 8.9×10^{-5} S cm^{-1} at 40 °C with 123 mAh g^{-1} and 91 mAh g^{-1} discharge capacities at 0.1 C and 0.5 C rates, respectively.[64] Most studies have been conducted using PEO polymer. However, some PEO-based ILGPEs are structurally unstable at high temperatures due to their low melting temperature (~56 °C). Thus, PEO-based ILGPEs are not feasible for high-temperature LIB applications.

In the current investigation, Singh's group used polymer poly(vinylidene fluoride-cohexafluoropropylene) (PVdF-HFP) due to its high excellent electrochemical stability, excellent mechanical strength, high thermal stability, high dielectric constant, ability to easily separate salts, simple thin film form and IL 1-ethyl-3-methylimidazolium bis(fluoromethyl sulfonyl)imide (EMIMFSI) because of its high ionic conductivity, low viscosity, and its good plasticizing effect. Lithium imide salt lithium bis(trifluoromethyl sulfonyl)imide (LiTFSI) has been chosen for its high thermal stability and low lattice energy so that it could be effectively disassociated into cations/anions. Lithium foil is considered as an anode due to its high energy density and lithium iron phosphate ($LiFePO_4$) is used as a conventional cathode substance for LMPBs due to the following advantages such as good thermal stability, higher discharge voltage base, lower electrolyte sensitivity, high capacity, low cost and non-toxicity. Here polymer electrolyte is not only used as a separator and more as an ion-conductor for transporting ions from anode to cathode or vice versa. The test indicates that even the 40wt. percent IL comprising GPE has a ΔT of ~3.8×10^{-4} at 25 °C and a peak ionic conductivity value of ~4.6×10^{-4} S cm^{-1} at 25 °C when the 60 wt.% EMIMFSI was introduced into the PVdF-HFP + 20 wt.% LiTFSI framework. Also, Fig. 2(c, d) shows the temperature dependence of the ion conductivity, which is reported to improve with temperature, as the segmental motion of the polymer chain rises and the mobility of the ions in the polymer matrix also continues to increase with the temperature increase. Maximum ΔT was gained from ~6.0×10^{-4} S cm^{-1} and ~9.8×10^{-4} S cm^{-1} at 50 °C at 40 wt.% and 60 wt.% of GPE-containing IL.

This work suggests the feasibility of DEMETFSI-based ionic liquid for effective use in high-performance lithium-oxygen batteries. Such morphological modifications are due to various electrochemical processes, which include Li_2O_2-growth both on the electrode surface and through the electrolyte. It produced a proof-of-concept, lithium-ion-oxygen battery, including a conversion/alloy dependent anode instead of lithium oxide. The cell provided a reversible capacity of 500 mAh g^{-1} with a working voltage of approximately 1.6 V, therefore a theoretical energy density of approximately 900 Wh kg^{-1} which is considered desirable for Li-ion battery devices.

N-butyl-N-methylpyrrolidinium bis(trifluoromethane-sulfonyl) imide ($PyR_{14}TFSI$) is particularly well suited for lithium-air batteries with low cathodic polarization and remarkable electrochemical performance. N, N-diethyl-N-(2-methoxyethyl)-N methylammonium bis(trifluoromethane-sulfonyl)imide (DEMETFSI), an IL with lower viscosity than the former, was also suggested for use as an electrolyte part for lithium-air batteries. Here, Hassoun's group applied this study by properly describing the electrolyte based on DEMETFSI in aspects of electrochemical and chemical stability, as well as the charge-discharge cycle in lithium-oxygen cells at different temperatures.[65] The increase in temperature has resulted in a change in the morphology of the Li_2O_2 deposited at the cathode and an improvement in cell energy efficiency. In addition, the suitability of the DEMETFSI-based electrolyte for use in lithium-ion-oxygen cells is conclusively demonstrated. This study describes a move forward in the development of feasible, IL-based lithium-oxygen batteries for new innovative energy storage systems.

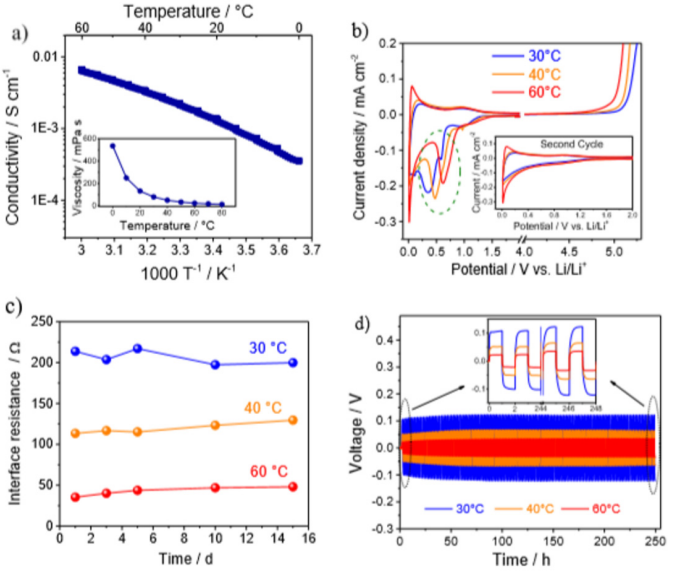

Fig. 1 (a) Arrhenius plot of the DEMETFSI-LiTFSI electrolyte with the viscosity vs. temperature plot (inset) (b) Current vs. potential plot of the LSV and of the CV performed on a Li/DEMETFSI LiTFSI/Super-C65 cell using a scan rate of 0.1 mV s^{-1} at various temperatures: 30 °C (blue), 40 °C (orange), 60 °C (red). (c) Time evolution of the interphase resistance of symmetrical Li/DEMETFSI-LiTFSI/Li at various temperatures: 30 °C (blue), 40 °C (orange), 60 °C (red). (d) Time evolution of the cell voltage and, in the inset, magnification of the 1st, 2nd, 123rd, and 124th cycle during stripping-deposition measurements performed on asymmetrical Li/DEMETFSI-LiTFSI/Li cell using a current of 0.1 mA cm^{-2} and a deposition-stripping time of 1 hour (Reproduced with permission from ref. 65).

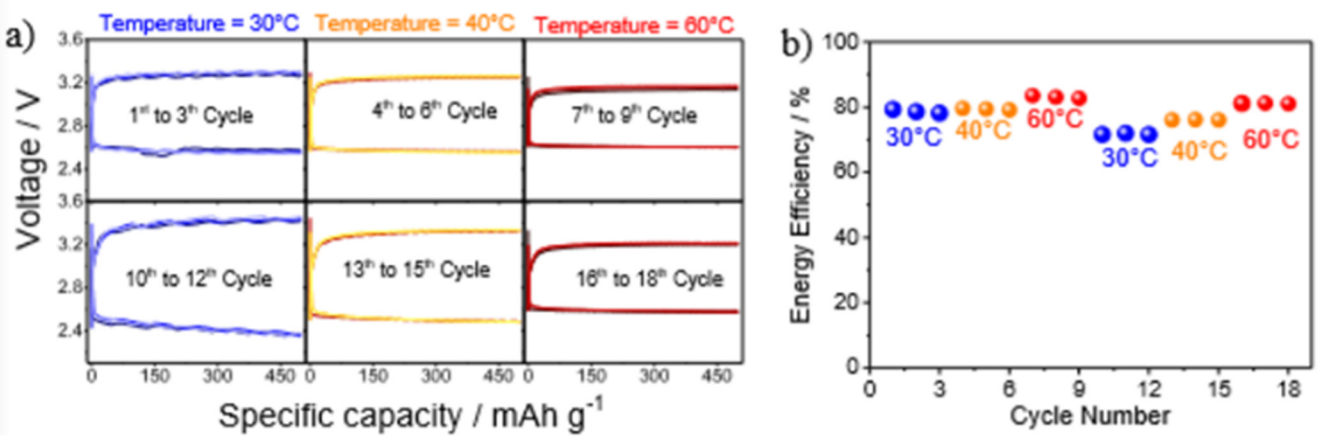

Fig. 2 Voltage profile (a) and energy efficiency upon cycling (b) of the Li/DEMETFSI, LiTFSI/O_2 cell cycled at various temperatures: 30 °C (blue), 40 °C (orange), 60 °C (red). Current density 50 mA g^{-1}. Capacity is limited to 500 $mAhg^{-1}$ (Reproduced with permission from ref. 65).

Fig. 1 demonstrates the electrochemical properties of the electrolyte DEMETFSI-LiTFSI. The Arrhenius plot at 0-60 ° C temperature range (Fig. 1a) shows a conductivity of 3.5 × 10^{-4} S cm^{-1} at 0 °C, which greatly enhances with a temperature of 2.2 × 10^{-3} S cm^{-1} at 30 °C, 3.4 × 10^{-3} S cm^{-1} at 40 °C and 6.6 × 10^{-3} S cm^{-1} at 60 °C, i.e. values considered suitable for high-performance lithium-oxygen batteries.[66] Fig Inset. 1a displays the viscosity of the electrolyte DEMETFSI-LiTFSI in the same temperature range. The graph illustrates a relatively high value at 0 °C (above 500 mPs) which quickly reduces by increasing temperatures to 30 ° C (80 mPs) and 60 °C (24 mPs) respectively. Conductivity and viscosity, consistent with the Walden law in this range of temperatures and working conditions,[67] differ from the linear Arrhenius-type behavior and are better understood in the Vogel-FulcherTammann (VFT) Model at the low-temperature domain.[68] A more detailed analysis, based on the VFT simulation, has previously been mentioned for this group of electrolytes within a larger temperature range.[69] The improvement in electrolyte conductivity at higher temperatures, directly attributable to the lowered viscosity, 21 is predicted to greatly improve the electrochemical performance of the system. The properties of the electrolyte have also been studied at various temperatures. Fig. 1b reports the electrochemical stability window of the carbon electrode at different temperatures., i.e., 30 °C (blue line) 40 °C (orange line) 60 °C (red line). The first cathodic scan shows a wide peak (circulated in green) which has no related peak in the next anodic scan. It is therefore correlated with the irreversible solid electrolyte interphase (SEI) formation on the carbon surface, which restricts further electrolyte decomposition during the following cycles. (see 2nd cycle in the inset of Fig. 1b). The permanent plateau correlated with the SEI development changes to higher potential values by growing the temperature from 0.4 V at 30 °C (blue curve) to 0.5 V at 40 °C (orange curve) and to 0.6 V at 60 °C (red curve). In addition, higher temperatures can lead to faster kinetics of the reductive forming of the SEI layer and improved electrolyte conductivity. As a result, electrolyte decomposition occurs at higher potentials. At the lowest temperature (30 °C), the anodized side of the SEI-formation point is detected, which may be linked to the introduction of the IL cation into the carbon prior to the formation of SEI. The limited range conditions used for cycling have already been proposed for lithium-oxygen cells as the optimal conditions for a stable, continuous charge/discharge procedure. The results suggest a stable trend and only slight impacts of repeated heating/cooling on cell results. In light of the higher capacity, the cell displays steady cycling activity and demonstrates the reduction of the polarization of the cells by increasing the temperature and thus enhancing energy efficiency. Hassoun's group believed that the positive effect of the temperature increase on cell energy efficiency could be due to enhanced kinetics of the process of deposit of electrochemical lithium peroxide, affecting both the direction of reaction and the structure of the products produced. Nevertheless, further investigation is still needed to make this aspect fully clear. The proof-of-concept cell has a discharge working voltage focused at approximately 1.6 V and provides a reversible capacity of approximately 500 mAh g^{-1} carbon, but with a reasonably high polarization mostly related to the reaction. Despite the need for long-term cycling, especially in the air rather than pure oxygen, the cell originally mentioned here may represent a promising and safe system for storing energy.

2.1.2. IL Gel in Sodium Metal Battery

When the demand for lithium rises, sodium becomes an excellent replacement. Because sodium is cheaper, greater in content, less toxic and has an energy density comparable to that. Organic capture of the liquid electrolytes in sodium batteries has been widely reported. But it also has some issues like toxicity, flammability, and potential leakage. Sodium metal is highly reactive to organic liquid electrolytes and suffers from severe sodium dendrite formation, a problem that could potentially lead to an explosion. So, gels or solid electrolytes were of interest, as they prevent dendrites

formation. IL gel is a classic electrochemical semi-solid energy storage device with good mechanical elasticity and high ionic conductivity. Due to its low cost and excellent conductivity of the impregnated IL gel we use commercial glass fiber separator in this present manuscript.[40] The IL N-propyl-N-methyl pyrrolidinium bis(Fluor sulfonyl)imide (C_3mpyrFSI) has been reported to have excellent thermal stability and electrochemical efficiency on sodium-based electrochemical instruments.[70-71] In addition, the use of this IL gel film in versatile sodium batteries based on carbon-coated sodium vanadium phosphate cathode content ($Na_3V_2(PO_4)_3$@C (abbreviated as NVP@C) was demonstrated, demonstrating the system's superior protection.

The silicon-based sodium metal battery's current density with a certain capacity is 92%. It has an efficiency of 99.9 % after 150-coulomb charge and discharge cycles at the current density of 1 C. In particular, at the end of the cycle, emissions appear to be getting more stable. This can be because silicon magnesium and NVP materials are highly stable. High supporting IL gel film stability and interface stability is also beneficial for improving circulation performance.[73] (Fig. 3). Electrochemical impedance spectroscopy (EIS) was conducted on new cells and 150 deep 1c (10^{-6}-10^{-2} Hz frequency) cycles to examine dynamic changes in the polymer gel electrolyte's interfacial resistance. It is important to note that the Nyquist curve at the intermediate frequency shows an extra half-circle after 150 cycles. It is well known that this particular electrolyte's SEI layer can form a uniform electrolyte and dense layer, making the anode side of the sodium plating/stripping more efficient. Thus, due to the forming of the SEI layer during the process, the extra semicircle created at high frequencies is. It is worth noting that the bulk resistance (the semi-circle intersection point to the x-axis, Rb), which is ascribed to the resistivity of the gel-electrolyte, does not change obviously after 150 cycles, implying that the cell's impedance response is ruled by the formation of the SEI layer and the transfer of charge occurring at the electrode/electrolyte interphase. A 6 cm × 4 cm laminated cell was assembled in the argon glove box to confirm the safety and flexibility of the SILGMs by sandwiching the SILGM NVP@C coated on aluminum foil and a sodium metal foil anode between normal plastic laminating film. It is constructed that the SILGMs could be an attractive option as a strong electrolyte, both as an electrolyte and as a separator for sodium batteries, even ideal for rolling to rolling output.[72]

2.1.3. IL Electrolytes for Sodium-Ion Batteries

Sodium has a deep, lithium-like source which makes it a good replacement. P2-layered transition metal oxide, consisting of two layers of the prism and MO_6 octahedron, displays greater phase stability through electrochemical sodiation and desodation in the cathode content of the sodium ion battery than other layered transition metal oxides. However, during the descaling process, the jantler distortion of manganese ions occurs which means that the cyclic stability of layered manganese oxides as cathode materials is not sufficient. In carbonate solvents (ethylene carbonate (EC), propylene carbonate (PC), dimethyl carbonate (DMC), etc.), the traditional sodium-ion battery electrolyte dissolves in sodium perchlorate.[73] However, in these traditional electrolytes, $NaMnO_2$ and its accessories display poor cyclic stability.[74-75] Recently IL electrolytes have been reported to improve the cyclic stability of the sodium ion battery cathode materials. This effect has been described to vary with varying sodium salts or levels. Hence the purpose of this paper is to study the influence of IL electrolyte-conductive salts composed of BMPTFSI solvent and various sodium salts on the cycling stability of cathode materials P2-$Na_{0.6}Co_{0.1}Mn_{0.9}O_{2+z}$ (NCO) ($0 \le z \le 0.25$).[76]

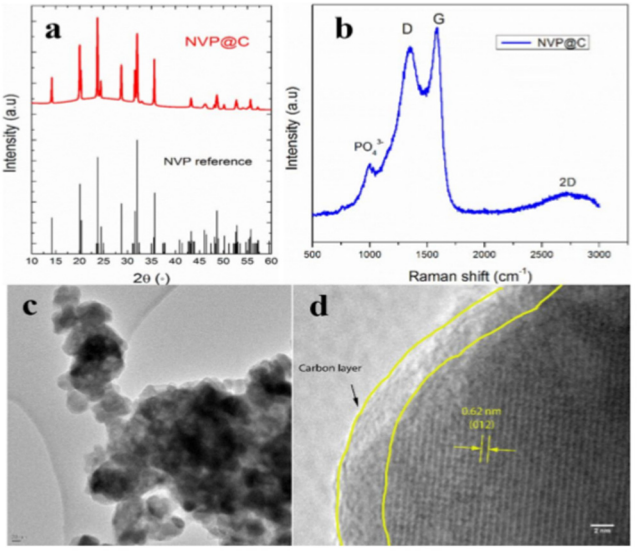

Fig. 3 XRD pattern (a) and Raman spectrum (b) of the as-synthesized NVP@C. TEM images: (c) low magnification, (d) HR-TEM (Reproduced with permission from ref. 73).

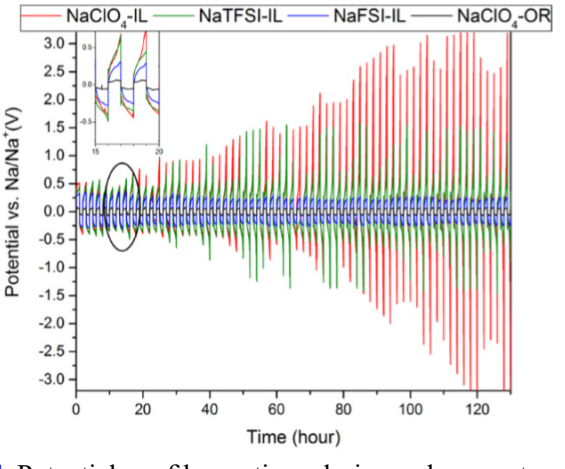

Fig. 4 Potential profile vs time during subsequent sodium stripping/plating behavior performed in the symmetric Na/electrolyte/Na cell at a current rate of 0.1 mA cm^{-2} and stripping/plating time of 1 h (Reproduced with permission from ref. 79).

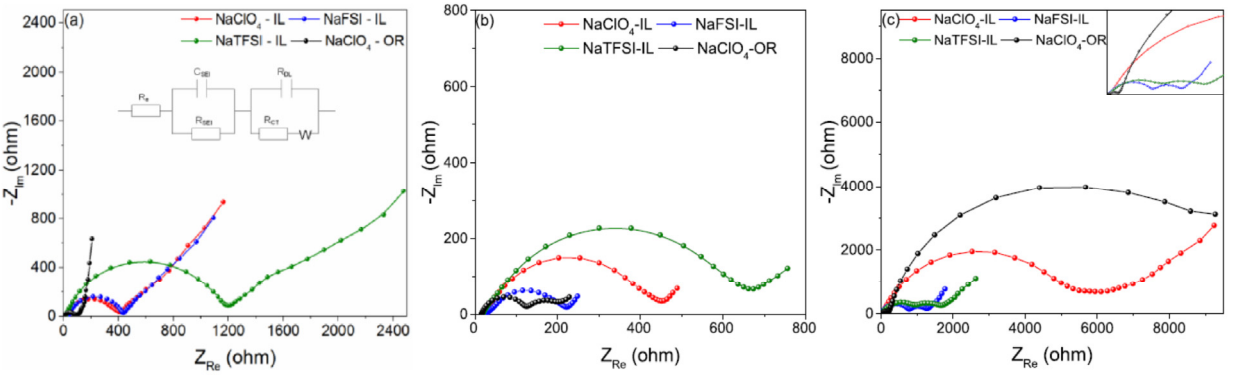

Fig. 5 Impedance spectra of NCO after 1 cycle (a), after 30 cycles (b), and after 500 cycles (c) (Reproduced with permission from ref. 79).

Overall, IL electrolyte conductivity is lower, and the viscosity is greater than that of the traditional $NaClO_4$-OR organic electrolyte.[77] As shown in Fig. 4 and Fig. 5, the conductivity and viscosity change with the salt carrying sodium. Among the three salts, $NaClO_4$ has had the greatest impact on IL electrolyte conductivity and viscosity. The electrolyte NaTFSI-IL has larger conductivity than NaFSI-IL. As a result, NaFSi-IL cells had the highest coulomb efficiency, around 100 percent, in terms of coulomb efficiency. $NaClO_4$-or battery has 98% coulomb efficiency. The coulomb output of the NaFSi-IL battery is also over 99 %, but the coulomb performance of the NaFSi-IL battery varies widely in the first 100 cycles, which may be correlated with some unavoidable side reactions while charging. $NaClO_4$-IL cells had the lowest coulomb efficiency of the measured electrolyte, about 92 %. The choice of sodium salt in IL electrolyte can be seen to have a significant effect on the coulomb efficiency. IL electrolytes' low rate performance can be explained by their high viscosity and low conductivity as compared with OR electrolytes. And they also discussed the properties of the CEI layer. It is evident that the shift of salt dissolved in the BMPTFSI IL results in the discrepancy in the properties of structure in the CEI ground (Fig. 6).

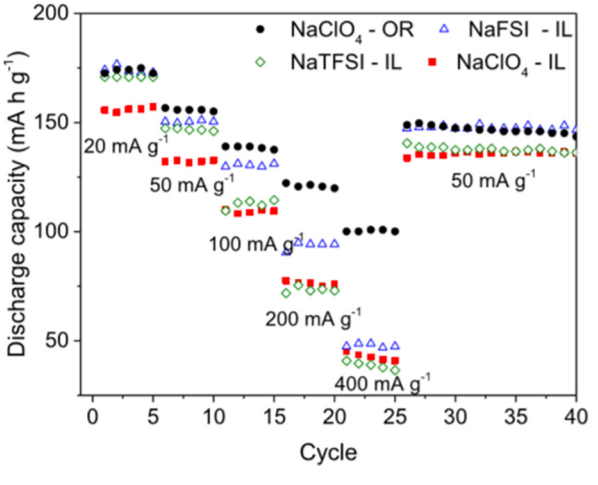

Fig. 6 Rate test performance at five different rates (Reproduced with permission from ref. 80).

The CEI layer structure is close to that of the SEI layer (that is when sodium is injected into the oxide). The cleavage of TFSI anion in $NaClO_4$-IL electrolyte (Fig. 7) occurs at the C-F bond.[78] No $NaClO_4$ has been decreased in the case of two other electrolytes, NaFSi-IL and NaFSi-IL, thus the above process may be unsuccessful. The observed components such as $CF_3SO_3N^-$, $CF_3SO_2N^-SO_2$, and NSO_2^- indicate, according to the XPS results, that N-S cleavage can occur (reaction 1).[79] These organic compounds can have a positive effect on long-term circulation.

2.1.4. Rechargeable aluminum ion batteries

Rechargeable aluminum ion batteries (RABs) are considered to be one of the most exciting rechargeable batteries of the next decade because Al is the most abundant metal product in the earth's crust.[80-84] But, the development of RABs has been hindered by two major bottlenecks: 1, Difficulty surrounds the design of a proper electrolyte with a wide electrochemical stability window; 2, Only a small proportion of cathode materials can intercalate and deintercalation the Al_3^+ ion reversibly. Graphite, due to its effective electrochemical intercalation $AlCl_4^-$ within graphite, has been proven to be an appropriate candidate.[85] Rani *et al*. used natural graphite fluorinated as a cathode in RABs, offering stable performance but delivering only low operating voltage.[86] Lin *et al*. have used a three-dimensional (3D) graphite foam as a cathode for RABs, indicating an operating voltage of 0.2 V.[87] Given the strong operating voltage, though, due to its low power (60 mAh g^{-1}), the graphic foam/Al battery can not meet the demand for high energy density applications. The high-capacity cathode element, iodine (211 mAh g^{-1}), has proved to be a suitable candidate in Li/I_2,[88] Zn/I_2,[89] and Mg/I_2[90] batteries.

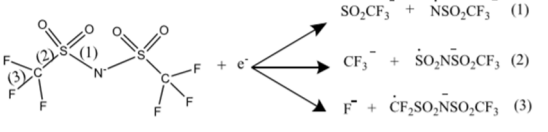

Fig. 7. Decomposition pathway of the TFSI anion (Reproduced with permission from ref. 80).

An Al/I_2 rechargeable battery is extremely attractive due to its high energy density, reasonable theoretical operating voltage, and low cost. A primary Al/I_2 battery and a combination of dye-sensitized solar cells (DSSC) based on AlI_3 electrolytes were first reported by Xue *et al*.[91] This primary Al/I_2 battery can unfortunately not be recharged. A rechargeable Al/I_2 battery is not reported mainly due to the obstacle of finding a suitable cathode based on iodine and highly reversible Al deposition−stripping electrolyte. The above reported an Al/I_2 rechargeable battery using the PVP-I_2 complex as a cathode and the IL as an electrolyte at room temperature. The hydrogen bonds between the PVP and the iodine element ensure highly reversible conversion reaction of the I_3^-/I^- redox pair in the cathode, effectively mitigating the polyiodide shuttle effect towards the Al anode. As shown in Fig. 8a, the iodine-based cathode undergoes a conversion reaction process in the Al/I_2 battery, triggering some kind of novel redox chemistry in RAB system design.

$$\text{Anode:}\quad 2Al + 14AlCl_4^- \underset{\text{charge}}{\overset{\text{discharge}}{\rightleftharpoons}} 8Al_2Cl_7^- + 6e^- \qquad (1)$$

Cathode:

$$8Al_2Cl_7^- + 6e^- + 2[P]^+I_3^- \underset{\text{charge}}{\overset{\text{discharge}}{\rightleftharpoons}} 2[P]AlI_3 + 14AlCl_4^- \qquad (2)$$

The mechanism of the rechargeable Al/I_2 battery can be written according to the above discussion
where P is PVP (polymeric matrix).

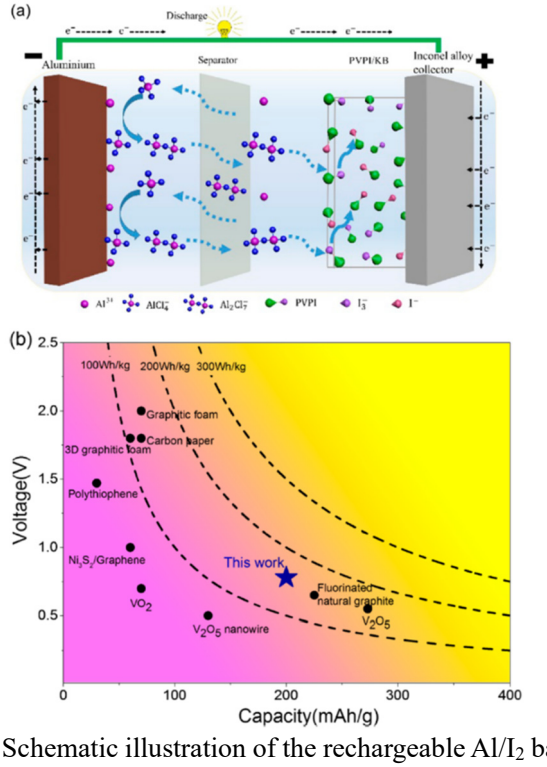

Fig. 8. Schematic illustration of the rechargeable Al/I_2 battery. (a) Schematic of rechargeable Al/I_2 batteries. (b) Capacity and voltage of the iodine cathode compared to reported rechargeable nonaqueous aluminum batteries (RABs) (Reproduced with permission from ref. 49).

It is reported that a rechargeable Al/I_2 battery is based on a PVP-I_2 cathode and an ionic liquid electrolyte for the first time. The rechargeable Al/I_2 battery is controlled by the conversion reaction mechanism as compared to the poor diffusion by intercalation in a traditional cathode in RABs. Due to the unique configuration of PVP-I_2 with hydrogen-bonding interaction, the shuttle effect of polyiodide could be greatly reduced in this method. Throughout long-term load cycling, the bond between the polymer PVP and the iodine portion may maintain the redox conversion reaction highly reversible in this method. The Al/I_2 rechargeable battery delivers a high capacity of > 200 mAh g^{-1}, corresponding to an energy density of > 150 Wh kg^{-1} (based on iodine mass) at 0.2 C (Fig. 8b), and excellent stability even after 150 cycles at 1C, which is one of the best RABs. The low cost, safe, and unique Al/I_2 rechargeable battery makes it a promising candidate for multivalent metal ion rechargeable batteries.

2.1.5. IL for Supercapacitor-battery

While electrochemical double layer capacitors (EDLCs) provide high power density, they typically only store a small fraction of the energy of the battery (< 30 percent). Both devices can benefit from combining the batteries with EDLCs. They are known as supercapacitor-battery combination. The focus of the group is to combine a sodium metal battery type electrode with a pseudo-capacitor electrode, which combines high energy density with high power density to allow quick charging and discharge. The simple synthesis (a one-step calcination process of starting materials) and the direct application of N, S co-doped mesoporous carbon material (NDMC) in symmetric supercapacitors have been documented recently. The NDMC material has a good porous structure which enables ions to easily spread through the carbon frame, resulting in a high capacity rate (high power density) and excellent capacity retention.[92] Taking into account the advantages of the sodium metal anode in energy storage devices (ESDs), the MacFarlane group has now introduced a supercapacitor based on sodium metal or battery hybrid (here called sodium hybrid) with the NDMC cathode.[93] This combination should result in a safety device with low costs, high capacity and high power density. In addition, the group presented a hybrid sodium metal-based device that uses an easily and cheaply produced carbon cathode. Stable and high rate cycling at both room temperature and 50 °C is demonstrated. The IL electrolyte ensures that the "supercapacitor-battery" shows much higher stability of cycling against sodium-metal than traditional electrolytes. The functionality of chemically bound sulfur within the cathode means that our device can exploit Na-S chemistry in the IL. The hybrid system could be regarded as a possible part of large-scale energy storage systems at both room temperature and 50 °C, due to its high efficiency at low and high load/discharge rates. The XPS analysis of the post-cycled electrodes demonstrates the concentration profile of carbon, sulfur and sodium across the whole etching profile.

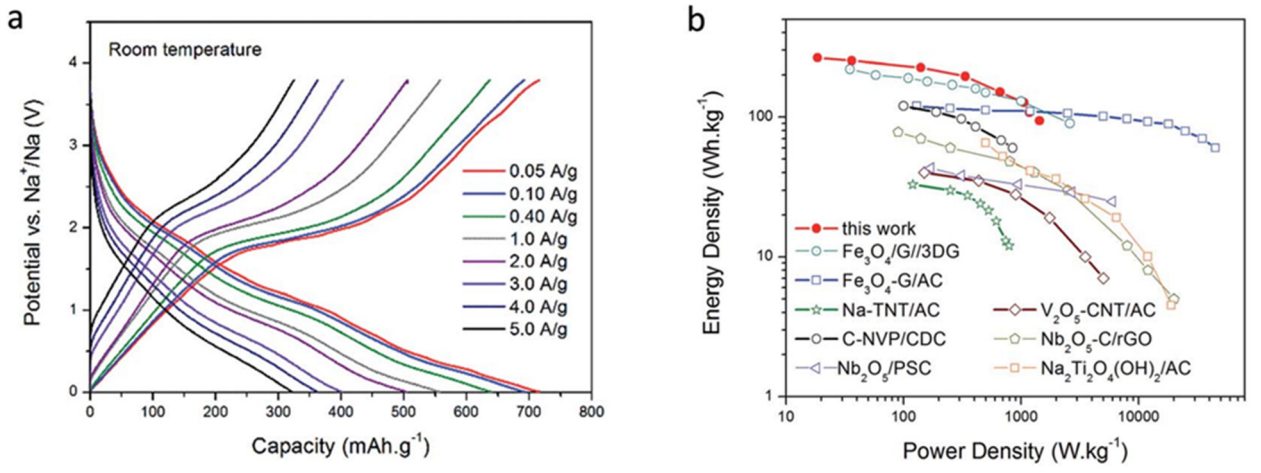

Fig. 9 (a). Voltage profiles at different current densities after 3,000 cycles at room temperature (b). Ragone plot comparing other Li/Na-ion based hybrid devices (all data at room temperature) (Reproduced with permission from ref. 93).

As shown in Fig. 9, these findings clearly show Na-S significant role in the NDMC-10 electrode's large capacity cycling.[93] It is also easy to produce, as the cathode content can be easily obtained from a straightforward process that does not require components of transition metals.

Mao *et al*. reported a method to prepare a high-performance solid-state electrolyte based on porous polybenzimidazole (pPBI) and IL ((1-(3-trimethoxysilylpropyl)-3-methylimidazo-lium chloride).[94] The obtained porous composite film electrolyte is assembled with an activated carbon electrode to prepare an all-solid-state supercapacitor (ASSC) (Fig. 10). The result of electrochemical performance displayed that ASSC has a specific capacitance of 85.5 F g^{-1} at 120 °C and keeps 91.0% capacitance and 95.8% coulomb efficiency after 10 000 constant current charges. IL could improve the ionic conductivity and mechanical properties of the electrolyte film.

2.2. Application of ILs in energy conversion

With the continuous depleting of fossil fuels and the development of global culture, much research have been interested in developing efficient energy conversion technologies. Particularly, the highly efficient electrocatalysts for the electrode reactions, such as oxygen evolution reaction (OER), oxygen reduction reaction (ORR) and hydrogen evolution reaction (HER). However, the high cost and low diffusion rate of gases towards the electrode limit their widespread applications. Recently, some workers reported that the use of IL as a non-volatile electrolyte or as a single-source precursor for the preparation of electrode materials, which could improve the efficiency and decrease the cost.[20,28] In the processes, ILs played three distinct roles viz. solvent, template, and catalyst. Later, Chaugule *et al*. reported IL-derived Co_3O_4-N/S- doped carbon catalysts for the enhanced OER. It demonstrated that the obtained Co_{10}-NS-C displayed excellent OER with a low overpotential of 350 and 270 mV at the current density of 10 mA cm^{-2} in 0.1 and 1 M KOH (Fig. 11).[95] It shows that the structural diversity of ILs could control properties and the defect structure of the carbon material.[96-97]

ILs have been widely used for ORR via the formation of a superoxide radical anion ($O_2^{\bullet-}$). The stability of $O_2^{\bullet-}$ could be affected by the IL cations, IL structures, and the electrode materials. It founds that the accumulating $O_2^{\bullet-}$ near the IL-electrode interface is affected by the affinity between the $O_2^{\bullet-}$ and IL cation. Zeng *et al*.[98] had reported an approach to study the facet effects of the ORR process in an ionic liquid 1-butyl-1-methylpyrrolidinium bis(trifluoromethylsulfonyl)imide ([Bmpy][NTf_2]). The results demonstrate the facet-dependence of oxygen reduction in an ionic liquid medium. Kuwabata and co-workers[99] reported an electropolymerization reaction which is observed at the thin ionic liquid (IL) layer between Pt nanoparticles and carbon support on Pt nanoparticle-modified carbon electrocatalysts prepared using an N, N-diethyl-N-methylammonium hydrogen sulfate ([DEMA][HSO_4]) protic IL with a [DPA][HSO_4] POS. The result shows that the Pt nanoparticle dispersed ILs enhanced catalytic performance. To understand the structuring of IL on the surfaces in the presence of oxygen or water is necessary.

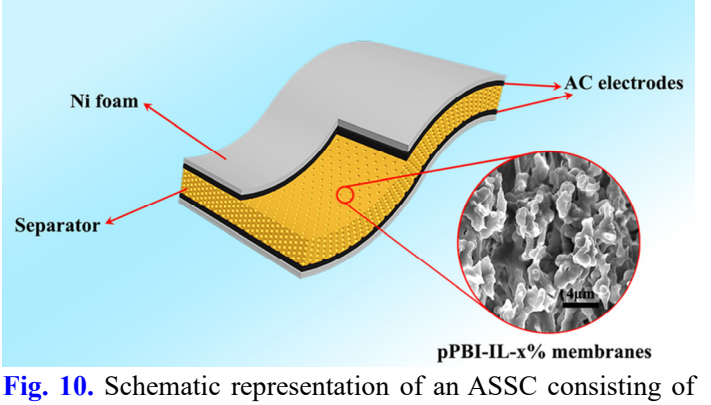

Fig. 10. Schematic representation of an ASSC consisting of the pPBI-IL-x% films and activated carbon electrodes (Reproduced with permission from ref. 94).

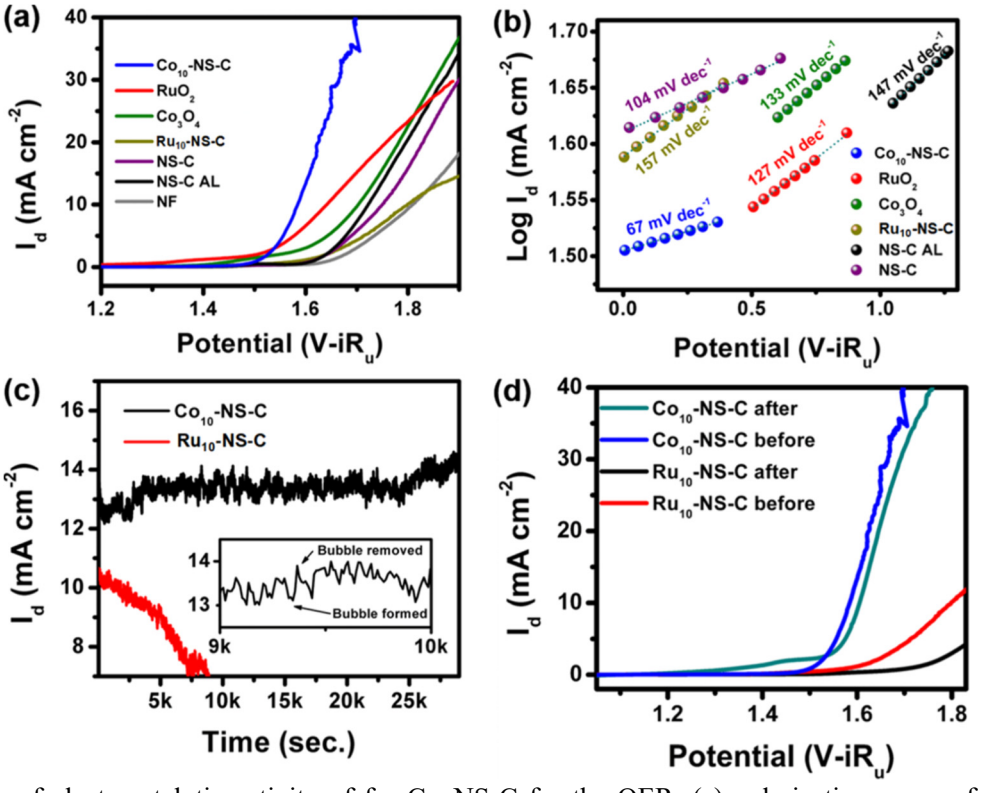

Fig. 11. Evaluation of electrocatalytic activity of for C_{10}-NS-C for the OER; (a) polarization curve of different catalysts collected at a scan rate of 0.2 mV s^{-1} in 0.1 M KOH, (b) Corresponding Tafel plots, (c) Chronopotentiometric curves, and (d) LSV curves collected before and after stability test (Reproduced with permission from ref. 96).

Silvester[100] reported that there is a significant amount of water incorporated at the electrode-RTIL interface in [C_2mim][NTf_2] and [$N_{4,1,1,1}$][NTf_2], but not in the more hydrophobic [$P_{14,6,6,6}$][NTf_2] and the presence of moisture has a significant impact on ORR currents in [C_2mim][NTf_2] even at extremely low humidity levels (Fig. 12).

2.3 Application of ILs for the conversion of CO_2

CO_2 as one kind of greenhouse gases is from burning fossil fuels and plays an important role in global climate change. The reduction of CO_2 emission or the utilization of CO_2 is necessary for human society. Yet, CO_2 with cheap and low toxic could be a source of carbon for organic chemicals such as carboxylic acids, organic carbonates, urea and fertilizers, and methanol. Up to now, there are many methods for the conversion of CO_2, such as photochemical, thermal and electrochemical. Electrochemical methods have gained much attention because the method is a low cost, compact, modular and easy to control different parameters such as potential, electrolyte and electrode materials. IL with high CO_2 solubility, intrinsic ionic conductivity, and wide potential windows have gained much attention as the solvent for CO_2 electroreduction. The electrochemical reduction of CO_2 could be generated CO,[101-103] methanol,[104] CH_4,[104-106] C_2H_4,[107] acetic acid/acetate,[108] as well as others via two-, four-, six-, and eight-electron reduction pathways in different electrolytes over metals, metal complexes, and non-metallic electrodes.[109-112]

Han *et al.*[113] studied the efficient reduction of CO_2 into formic acid in the IL catholyte mixture. They found that the addition of the small amount of H_2O to IL/acetonitrile electrolyte mixture could enhance the efficiency of the electrochemical reduction of CO_2 into formic acid (HCOOH) on a Pb or Sn electrode, Fig. 13 shows the effect of applied potential and H_2O content in the ternary mixture. Using [Bmim]PF_6 (30 wt.%)/AcN-H_2O (5 wt.%) as the electrolyte, current densities as high as 37 and 32 $mAcm^{-2}$ and faradaic efficiencies as high as 91.6 and 92.0%, were reached on a Pb and Sn electrode, respectively.

Hardacre *et al.*[114] reported a new low-energy pathway for the electrochemical reduction of CO_2 to formate and syngas at low overpotentials, using IL as the solvent. The results show that super-basic tetraalkyl phosphonium IL [P_{66614}][124Triz] can chemisorb CO_2 through equimolar binding of CO_2 with the 1,2,4-triazole anion and the overpotentials for CO_2 reduction to form formate is as low as 0.17 V at silver electrodes. However, using [P_{66614}][124Triz] with physically absorbed CO_2 or [P66614][NTf_2] with chemisorption, the overpotentials increase and only CO as the product. It may be due to the reactive anions that can provide a new low energy pathway for CO_2 electroreduction.

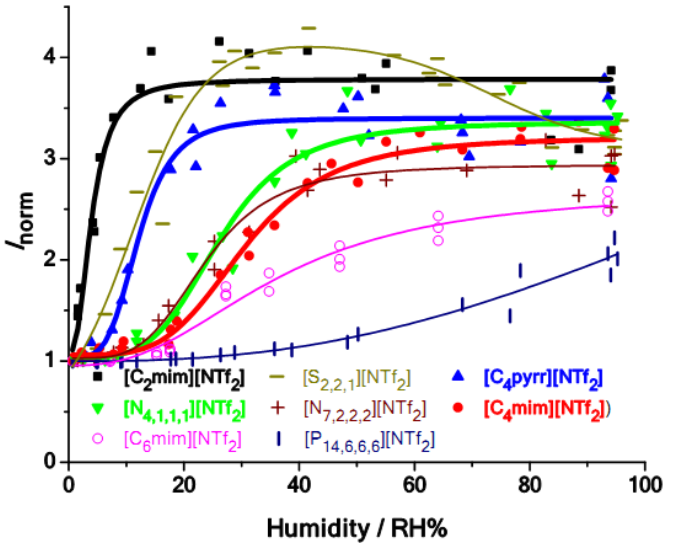

Fig. 12. Effect of humidified environments on the normalized current for oxygen reduction in $[C_2mim][NTf_2]$ (■), $[S_{2,2,1}][NTf_2]$ (—), $[C_4mpyrr][NTf_2]$ (▲), $[C_4mim][NTf_2]$ (•), $[N_{4,1,1,1}][NTf_2]$ (▼), $[N_{7,2,2,2}][NTf_2]$ (+), $[C_6mim][NTf_2]$ (○) and $[P_{14,6,6,6}][NTf_2]$ (|) with increasing relative humidity percentage (RH%). CVs at 100 mV s^{-1} were carried out on Pt-TFEs and each scan was taken after 45 min equilibration time. The scans were taken at 100 mVs-1 and with a step potential of -2.5 mV[99] (Reproduced with permission from ref. 99).

Dimethyl carbonate (DMC) has attracted much attention as an environment-friendly intermediate for organic synthesis and an option for meeting the oxygenate specifications on gasoline. Recently, electrochemical activation of CO_2 in the ionic liquid is considered to be an effective route for synthesis DMC. In these methods, the electrolysis experiments are carried out by constant-potential electrolysis in an undivided cell under mild conditions without any toxic solvents, catalysts and supporting electrolytes. Importantly, the ILs could be recyclable. The yield could be affected by the temperature, working potential, electrode material, the structure of IL, reactant concentration and the passed charge.[110-112,115]

3. Future Directions and Perspectives

3.1 Computational simulation for IL Electrolyte Systems

With climate destruction and fossil fuel depletion people need to find a sustainable process. That is what hydrogen does a good job. The hope is to make hydrogen, such as fuel cells, more effective in renewable and zero-emission systems. Due to its unique properties, such as low volatility, high ionic conductivity and wide range of liquid phase, ILs are expected to be used as an electrolyte as a kind of liquid salt at medium temperature. Umebayashi and colleagues suggest a cave-like mechanism for the conduction of protons where proton transitions commonly occur between ions and neutral particles without barriers to high energy.[116-117] Protons transmit charges through this mechanism through an extended three-dimensional network of hydrogen bonds, which enables them to disperse at a relatively high level. They analyzed the possible proton hopping paths and addressed the mechanism's structural key elements. AIMD simulation is especially suited for spontaneous occurrences. The density values of the climhoac mixture can be found differing in the literature.[118] Utilizing different densities they set up two simulation groupings. They constructed three different boot settings, one consisting solely of ions, the only one in neutral colors, called n-methylimidazole and acetic acid (called neuro membrane), and one mole 50:50 neutral and ionic mixture. The easiest method of transporting protons is the carrier system, where protons are transported by molecules or cations serving as "carriers." The proton's conductivity is then constrained by the rate of diffusion from the carrier.[119] By shifting the ex-bond in favor of hydrogen bond networks the Grotthuss mechanism bypasses this problem. The quick passage of certain small particles can often be done by pushing the pore in the liquid, although these are expressed in the quicker actions of small particles to diffuse. Through AIMD models, an imidazole, anion, and proton, we can gather information about the diffusion behavior of different species in the system. Based on all the outcomes mentioned in this article, including direct visualization of the process of transferring protons, it can say that the balance of the mixture studied includes continuous protons exchange between ions and neutral species. The system has many mechanisms for proton transfer which have synergistic effects.

The perfect procedure for proton conduction in energy unit electrolytes is a cavern-like dispersion component that favors much slower vehicle instruments. For glorious dissemination to happen, in any case, the vitality obstruction for proton move must be lower. They considered the elements of proton move between n-methylimidazole positive particles and acetic acid derivation anions and found that initiation obstructions could be overlooked and effectively defeat in fluid frameworks. This is the reason there is such astounding proton action in the reproductions. Low DpKa frameworks can display high ionic conductivity through the grotthuss-like proton conduction instrument, while high DpKa PILs cannot. These frameworks are for the most part maintained a strategic distance from in light of the fact that they display poor thermal dependability and higher unpredictability than high DpKa PILs. By the by, there is potential to distinguish profoundly conductive media by structuring objective guided tests with low vitality proton move boundaries. Right now, they have gathered and given data that will help accomplish this objective. Grotthuss dispersion method in PILs has incredible potential and merits further examination.

3.2 Cellulose ionic conductors

Poor quality thermal force age has pulled in enthusiasm for a considerable length of time. Petroleum derivatives, atomic force age and modern procedures, and sun-oriented thermals are basic second-rate heat sources.

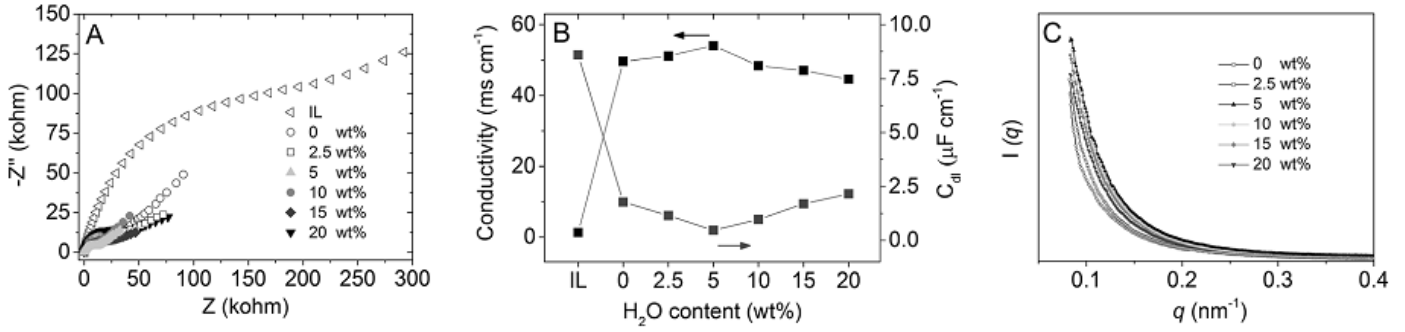

Fig. 13. Effect of H_2O content in a [Bmim]PF_6(30 wt.%)/AcN-H_2O mixture. A) Nyquist plots for a Pb electrode in various electrolytes; B) conductivities and double-layer capacitance of [Bmim]PF_6 (30 wt.%)/AcN-H_2O mixtures containing different amounts of H_2O (AcN basis); C) SAXS curves of [Bmim]PF_6 (30 wt.%)/AcN-H_2O with different amounts of H_2O (AcN basis)[112](Reproduced with permission from ref. 112).

Be that as it may, just the Kalina cycle, natural Rankine cycle and thermoelectric impact are utilized to change over poor-quality thermal sources into electricity. The adaptable use of these procedures in heat recuperation is to a great extent problematic. The analyses, which depend on probes natural materials, can be adaptable and can be spent on minimal effort arrangements. The distinction in thermal portability between electrolyte anions and particles is the way to amplify the utilization of thermal produced electrical signs. Accordingly, there has been ongoing hypothetical guess of utilizing accused nanochannels of an articulated electric twofold layer for the program the age of the thermally produced voltage. Hu's gathering's work exhibits a critical increment in the electrothermal pressure created by osmosis.[120-125] The electrolyte enters the cellulose film by improving the selectivity and cooperative energy of particles in the charged atomic chain. The development of cellulose II in the subsequent film prompts Na - cellulose complex arrangement after electrolyte invasion. Oxidation of 2,2,6 - tetramethylpiperidine-1-oxyl (TEMPO) upgrades the negative charge thickness of the cellulose nanofibres, which prompts extra improvement in the thermally produced voltage. As shown in Fig. 14 and 15, Hu's gathering's proposed wood-based ionic conductor is additionally adaptable, conceptual a progression of potential uses of particle specific cellulose films have prospected, including temperature detecting and poor quality thermal vitality assortment.[126]

The SEM picture shows the wood cells (i.e., veins and fiber tracheid) vertically properties. Use SANS included (Fig. 15), It estimated the fundamental fiber distance across of film for ~ 4 nm. The thermal rate is 10 °C min^{-1} when the thermo-gravimetric investigation indicated that the cellulose layer at 315 °C in great thermal soundness. They surveyed the nanofluids of cellulose film execution. In such a little convergence of sodium hydroxide, the conductivity is consistent (totally controlled by the fixed charge on the cellulose), for example, electrical conductivity and salt fixation reliance of level. So as to comprehend the connection between the structure and execution, we assessed the thermal voltage, and the structure of various kinds of the film has carried on the extensive examination, including regular wood, unadulterated cellulose type I variation to remove the lignin and cellulose layer type II variation to remove the lignin layer. The watched heat produced voltage is driven by temperature-related electrophoresis particle development brought about by particular particle dispersion, which is typically not is believed to be engaged with the conventional thermoelectric case of structure designing.

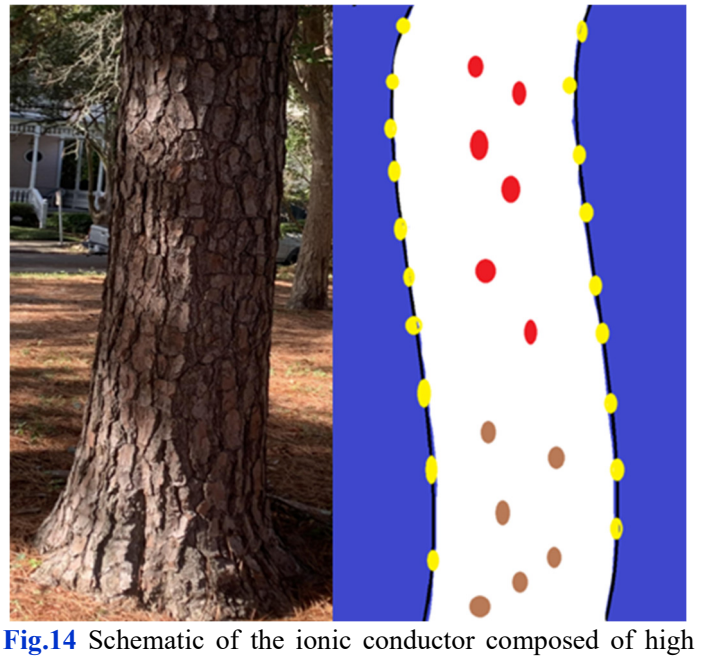

Fig.14 Schematic of the ionic conductor composed of high aspect ratio, aligned cellulose nanofibres. **(Left)**, the cellulose fibers are naturally aligned along the tree growth direction (white arrow). Cellulose exhibits a hierarchical alignment, in which the nanofibres consist of aligned cellulose molecular chains. **(Right)**, Schematic of the ionic device after infiltrating electrolyte into the nanofluidic cellulosic membrane. Under a thermal bias, the surface charged nanofibers regulate ionic movement via nanofluidic effects (that is, the overall effect created by a high degree of confinement and the charged walls of the cellulose nanochannels) (Modified from ref. 127).

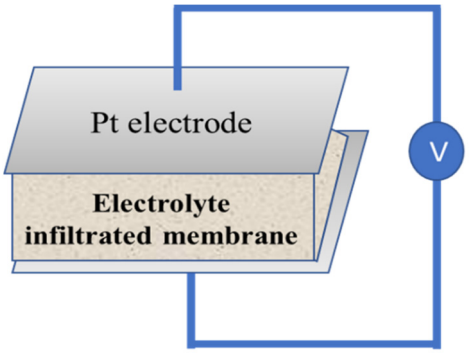

Fig. 15 Schematic of the testing setup for the nanofluidic ionic device, where the oxidized cellulosic membrane is infiltrated with polymer electrolyte and sandwiched between two platinum electrodes (Modified from ref. 127).

Ionic thermal charging practices. The more drawn out the release time of the cellulose layer, the more prominent the charge put away in the nanofluid film under a similar outside thermal predisposition. Run of the mill nanofluidic gadgets is manufactured by base up get together of low-dimensional structures or top-down scoring. Our technique maintains a strategic distance from these customary, however costly miniaturized scale/nano producing forms, utilizing basically adjusted cellulose nanofibers extricated from common wood. To exhibit extensibility, Hu's gathering built up a 10 cm^2 nanofluid layer that holds extraordinary adaptability because of its mesoporous structure acquired from regular wood. This adaptable cellulose film gives poor quality thermal assortment to control age.

4. Conclusion

ILs as "green solvents or electrolyte" has been designed for many applications via tuning their properties. In this review, we have given an overview of the ILs for the green electrochemistry application. The combination of electrochemical and ILs will be a potential filed. The good property of IL or IL-based composite materials with simple preparation procedures will promote the development of the electrochemical device and the conversion of CO_2. Taking advantage of the ILs could promote the electron transfer to nearby the electrode provides a good platform for the electrocatalysis and electrochemical synthesis. However, there is still a technical challenge to bring the device or the method in practical applications. To understand the fundamental electrochemistry of these electrochemical reactions, the role of ILs and the choice of electrode material will improve the property of the device and expand the application of ILs. A combination of IL with simulation computation, electrochemistry, and material chemistry will broaden the range of the electrochemical methods. In the last five years, many new reports are emerging providing new avenues for future research. The computational design has been involved in the IL-based systems by more understanding has achieved. It notes that the new ionic conductors produced from the natural material such as the cellulose have been attracted more attention currently with the potential to use as the next generation green materials.

Acknowledgments

This publication was made possible by the supports from the Army Research Office under Grant Number W911NF-18-1-0458, National Science Foundation (CHE-1832167, HRD-1700429, and HRD-1505219) and NIH (1R15GM113193-01, 5G12MD007595, 8UL1GM118967).

Conflict of Interest

There is no conflict of interest.

Supporting Information

Not Applicable.

References

[1] A. Midilli, I. Dincer and M. Ay, *Energ. Policy*, 2006, **34(18)**, 3623-3633, doi: 10.1016/j.enpol.2005.08.003.
[2] L. Gibson, E. N. Wilman and W. F. Laurance, *Trends ecol. Evol.*, 2017, **32(12)**, 922-935, doi: 10.1016/j.tree.2017.09.007.
[3] M. A. Green and S. P. Bremner, *Nat. Mater.*, 2016, **16(1)**, 23-34, doi: 10.1038/nmat4676.
[4] S. Chu, Y. Cui and N. Liu, *Nat. Mater.*, 2016, **16(1)**, 16-22, doi: 10.1038/nmat4834.
[5] T. Morstyn, N. Farrell, S. J. Darby and M. D. McCulloch, *Nat. Energy*, 2018, **3(2)**, 94-101, doi: 10.1038/s41560-017-0075-y.
[6] M. Bystrzanowska, F. Pena-Pereira, Ł. Marcinkowski and M. Tobiszewski, *Ecotox. Environ. Safe.*, 2019, **174**, 455-458, doi: 10.1016/j.ecoenv.2019.03.014.
[7] J. Byrne, *Green energy economies: The search for clean and renewable energy*, New York: Routledge; 1st Edition, 2017.
[8] K. M. Keramitsoglou, R. C. Mellon, M. I. Tsagkaraki and K. P. Tsagarakis, *Renew. Sust. Energ. Rev.*, 2016, **59**, 1332-1337, doi: 10.1016/j.rser.2016.01.005.
[9] A. M. A. Asiri and S. Kanchi, *Green Sustainable Process for Chemical and Environmental Engineering and Science: Ionic Liquids as Green Solvents*, New York: Elsevier, 1st Edition, 2019.
[10] F. Creutzig, P. Agoston, J. C. Goldschmidt, G. Luderer, G. Nemet and R. C. Pietzcker, *Nat. Energy*, 2017, **2(9)**, 17140, doi: 10.1038/nenergy.2017.140.
[11] E. Lachapelle, R. MacNeil and M. Paterson, *New Polit. Econ.*, 2017, **22(3)**, 311-327, doi: 10.1080/13563467.2017.1240669.
[12] M. Kar, O. Tutusaus, D. R. MacFarlane and R. Mohtadi, *Energ. Environ. Sci.*, 2019, **12(2)**, 566-571, doi: 10.1039/c8ee02437e.
[13] R. D. Rogers and K. R. Seddon, *Science*, 2003, **302(5646)**, 792-793, doi: 10.1126/science.1090313.
[14] J. M. Gomes, S. S. Silva and R. L. Reis, *Chem. Soc. Rev.*, 2019, **48(15)**, 4317-4335, doi: 10.1039/c9cs00016j.
[15] T. Welton, *Chem. Rev.*, 1999, **99(8)**, 2071-2083, doi:

10.1021/cr980032t.
[16] M. J. Earle, J. M. Esperança, M. A. Gilea, J. N. C. Lopes, L. P. Rebelo, J. W. Magee, K. R. Seddon and J. A. Widegren, *Nature*, 2006, **439(7078)**, 831-834, doi: 10.1038/nature04451.
[17] P. Wasserscheid and W. Keim, *Angew. Chem. Int. Edit.*, 2000, 39(21), 3772-3789, doi: 10.1002/1521-3773(20001103)39:21<3772::AID-ANIE3772>3.0.CO;2-5.
[18] Z. Wang, M. Guo, X. Mu, S. Sen, T. Insley, A. J. Mason, P. Král and X. Zeng, *Anal. Chem.*, 2016, **88(3)**, 1959-1964, doi: 10.1021/acs.analchem.5b04677.
[19] M. J.Earle and K. R. Seddon, *ACS Sym. Ser.*, 2002, **819**, 10-25, doi: 10.1021/bk-2002-0819.ch002.
[20] M. Armand, F. Endres, D. R. MacFarlane, H. Ohno and B. Scrosati, *Nat. Mater*. 2009, 8, 621-629, doi: 10.1038/nmat2448.
[21] C. A. Angell, Y. Ansari and Z. Zhao, *Faraday Discuss.*, 2012, **154**, 9-27, doi: 10.1039/c1fd00112d.
[22] X. Zeng and Z. Wang, (United States, 2015), pp. US Patent 9150971.
[23] Z. Wang, P. Lin, G. A. Baker, J. Stetter and X. Zeng, *Anal. Chem.*, 2011, **83(18)**, 7066-7073, doi: 10.1021/ac201235w.
[24] Y. Tang, Z. Wang, X. Chi, M. D. Sevilla and X. Zeng, *J. Phys. Chem. C*, 2016, **120(2)**, 1004-1012, doi: 10.1021/acs.jpcc.5b09777.
[25] C. M. Gordon, *Appl. Catal. A-Gen.*, 2001, **222(1-2)**, 101-117, doi: 10.1016/S0926-860X(01)00834-1.
[26] K. R. Seddon, *Nat. Mater.*, 2003, **2(6)**, 363-365, doi: 10.1038/nmat907.
[27] C. Arbizzani, M. Biso, D. Cericola, M. Lazzari, F. Soavi and M. Mastragostino, *J. Power Sources*, 2008, **185(2)**, 1575-1579, doi: 10.1016/j.jpowsour.2008.09.016.
[28] S. Zhang, J. Sun, X. Zhang, J. Xin, Q. Miao and J. Wang, *Chem. Soc. Rev.*, 2014, **43(22)**, 7838-7869, doi: 10.1039/c3cs60409h.
[29] S. Li, C. Yang, S. Sarwar, A. Nautiyal, P. Zhang, H. Du, N. Liu, J. Yin, K. Deng and X. Zhang, *Adv. Compos. Hybrid. Mater.*, 2019, **2(2)**, 279-288, doi: 10.1007/s42114-019-00103-w.
[30] M. Watanabe, M. L. Thomas, S. Zhang, K. Ueno, T. Yasuda and K. Dokko, *Chem. Rev.*, 2017, **117(10)**, 7190-7239, doi: 10.1021/acs.chemrev.6b00504.
[31] G. Gebresilassie Eshetu, M. Armand, B. Scrosati and S. Passerini, *Angew. Chem. Int. Edit.*, 2014, **53(49)**, 13342-13359, doi: 10.1002/anie.201405910.
[32] M. H. Chakrabarti, F. S. Mjalli, I. M. AlNashef, M. A. Hashim, M. A. Hussain, L. Bahadori and C. T. J. Low, *Renew. Sust. Energ. Rev.*, 2014, **30**, 254-270, doi: 10.1016/j.rser.2013.10.004.
[33] A. Basile, M. Hilder, F. Makhlooghiazad, C. Pozo-Gonzalo, D. R. MacFarlane, P. C. Howlett and M. Forsyth, *Adv. Energy Mater.*, 2018, **8(17)**, 1703491, doi: 10.1002/aenm.201703491.
[34] L. Lu, X. Han, J. Li, J. Hua and M. Ouyang, *J. Power Sources*, 2013, **226**, 272-288, doi: 10.1016/j.jpowsour.2012.10.060.
[35] S. S. Zhang, *J. Power Sources*, 2006, **162(2)**, 1379-1394, doi: 10.1016/j.jpowsour.2006.07.074.
[36] N. Alias and A. A. Mohamad, *J. Power Sources*, 2015, **274**, 237-251, doi: 10.1016/j.jpowsour.2014.10.009.
[37] D. Kumar, S. K. Rajouria, S. B. Kuhar and D. Kanchan, *Solid State Ionics*, 2017, **312**, 8-16, doi: 10.1016/j.ssi.2017.10.004.
[38] A. Manthiram and X. Yu, *Small*, 2015, **11(18)**, 2108-2114, doi: 10.1002/smll.201403257.
[39] T. H. Hwang, D. S. Jung, J. S. Kim, B. G. Kim and J. W. Choi, *Nano Lett.*, 2013, **13(9)**, 4532-4538, doi: 10.1021/nl402513x.
[40] S. K. Singh, L. Balo, H. Gupta, V. K. Singh, A. K. Tripathi, Y. L. Verma and R. K. Singh, *Energy*, 2018, **150**, 890-900, doi: 10.1016/j.energy.2018.03.024.
[41] L. Balo, H. Gupta, S. K. Singh, V. K. Singh, A. K. Tripathi, N. Srivastava, R. K. Tiwari, R. Mishra, D. Meghnani and R. K. Singh, *J. Solid State Electr.*, 2019, **23(8)**, 2507-2518, doi: 10.1007/s10008-019-04321-6.
[42] Q. Yang, Z. Zhang, X. G. Sun, Y. S. Hu, H. Xing and S. Dai, *Chem. Soc. Rev.*, 2018, **47(6)**, 2020-2064, doi: 10.1039/c7cs00464h.
[43] N. Jayaprakash, S. Das and L. Archer, *Chem. Commun.*, 2011, **47(47)**, 12610-12612, doi: 10.1039/c1cc15779e.
[44] S. C. Jung, Y. J. Kang, D. J. Yoo, J. W. Choi and Y. K. Han, *J. Phys. Chem. C*, 2016, **120(25)**, 13384-13389, doi: 10.1021/acs.jpcc.6b03657.
[45] T. Cai, L. Zhao, H. Hu, T. Li, X. Li, S. Guo, Y. Li, Q. Xue, W. Xing and Z. Yan, *Energ. Environ. Sci.*, 2018, **11(9)**, 2341-2347, doi: 10.1039/c8ee00822a.
[46] J. V. Rani, V. Kanakaiah, T. Dadmal, M. S. Rao and S. Bhavanarushi, *J. Electrochem. Soc.*, 2013, **160(10)**, A1781-A1784, doi: 10.1149/2.072310jes.
[47] M. Angell, C. J. Pan, Y. Rong, C. Yuan, M. C. Lin, B. J. Hwang and H. Dai, *P. Natl. Acad. Sci. USA*, 2017, **114(5)**, 834-839, doi: 10.1073/pnas.1619795114.
[48] H. Wang, S. Gu, Y. Bai, S. Chen, F. Wu and C. Wu, *ACS Appl. Mater. Inter.*, 2016, **8(41)**, 27444-27448, doi: 10.1021/acsami.6b10579.
[49] H. Tian, S. Zhang, Z. Meng, W. He and W. Q. Han, *ACS Energy Lett.*, 2017, **2(5)**, 1170-1176, doi: 10.1021/acsenergylett.7b00160.
[50] M. Que, Y. Tong, G. Wei, K. Yuan, J. Wei, Y. Jiang, H. Zhu and Y. Chen, *J. Mater. Chem. A*, 2016, **4(37)**, 14132-14140, doi: 10.1039/c6ta04914a.
[51] J. M. Armand, M. J. Chabagno, and M. J. Duclot. in Fast Ion Transport in Solids, PI Vashishta, J. N. Mundy, and G. K. Shenoy, 1979, pp. 131–136.
[52] Y. Zhu, S. Xiao, Y. Shi, Y. Yang, Y. Hou and Y. Wu, *Adv. Energy Mater.*, 2014, **4(1)**, 1300647, doi: 10.1002/aenm.201300647.
[53] J. Zhang, L. Yue, P. Hu, Z. Liu, B. Qin, B. Zhang, Q. Wang, G. Ding, C. Zhang, X. Zhou, J. Yao, G. Cui and L. Chen, *Sci. Rep-UK*, 2014, **4**, 6272, doi: 10.1038/srep06272.
[54] S. Das and A. Ghosh, *Electrochim. Acta*, 2015, **171**, 59-

65, doi: 10.1016/j.electacta.2015.04.178.
[55] K. Marsh, J. Boxall and R. Lichtenthaler, *Fluid Phase Equilibr.*, 2004, **219(1)**, 93-98, doi: 10.1016/j.fluid.2004.02.003.
[56] M. P. Singh, R. K. Singh and S. Chandra, *Prog. Mater. Sci.*, 2014, **64**, 73-120, doi: 10.1016/j.pmatsci.2014.03.001.
[57] H. Matsumoto, H. Sakaebe and K. Tatsumi, *J. Power Sources*, 2005, **146(1-2)**, 45-50, doi: 10.1016/j.jpowsour.2005.03.103.
[58] D. W. Kim, S. Sivakkumar, D. R. MacFarlane, M. Forsyth and Y. K. Sun, *J. Power Sources*, 2008, **180(1)**, 591-596, doi: 10.1016/j.jpowsour.2008.01.071.
[59] M. Galiński, A. Lewandowski and I. Stępniak, *Electrochim. Acta*, 2006, **51(26)**, 5567-5580, doi: 10.1016/j.electacta.2006.03.016.
[60] L. Liu, P. Yang, L. Li, Y. Cui and M. An, *Electrochim. Acta*, 2012, **85**, 49-56, doi: 10.1016/j.electacta.2012.08.066.
[61] M. Safa, A. Chamaani, N. Chawla and B. El-Zahab, *Electrochim. Acta*, 2016, **213**, 587-593, doi: 10.1016/j.electacta.2016.07.118.
[62] G. T. Kim, G. B. Appetecchi, F. Alessandrini and S. Passerini, *J. Power Sources*, 2007, **171(2)**, 861-869, doi: 10.1016/j.jpowsour.2007.07.020.
[63] L. Li, J. Wang, P. Yang, S. Guo, H. Wang, X. Yang, X. Ma, S. Yang and B. Wu, *Electrochim. Acta*, 2013, **88**, 147-156, doi: 10.1016/j.electacta.2012.10.018.
[64] C. Zhu, H. Cheng and Y. Yang, *J. Electrochem. Soc.*, 2008, **155(8)**, A569-A575, doi: 10.1149/1.2931523.
[65] U. Ulissi, G. A. Elia, S. Jeong, F. Mueller, J. Reiter, N. Tsiouvaras, Y. K. Sun, B. Scrosati, S. Passerini and J. Hassoun, *Chemsuschem*, 2018, **11(1)**, 229-236, doi: 10.1002/cssc.201701696.
[66] K. Xu, *Chem. Rev.*, 2014, **114(23)**, 11503-11618, doi: 10.1021/cr500003w.
[67] C. Schreiner, S. Zugmann, R. Hartl and H. J. Gores, *J. Chem. Eng. Data*, 2010, **55(5)**, 1784-1788, doi: 10.1021/je900878j.
[68] H. Ohno, *Electrochemical aspects of ionic liquids*. John Wiley & Sons: 2005.
[69] G. A. Elia, U. Ulissi, S. Jeong, S. Passerini and J. Hassoun, *Energ. Environ. Sci.*, 2016, **9(10)**, 3210-3220, doi: 10.1039/c6ee01295g.
[70] T. C. Mendes, F. Zhou, A. J. Barlow, M. Forsyth, P. C. Howlett and D. R. MacFarlane, *Sustainable Energy & Fuels*, 2018, **2(4)**, 763-771, doi: 10.1039/c7se00547d.
[71] M. Forsyth, H. Yoon, F. Chen, H. Zhu, D. R. MacFarlane, M. Armand and P. C. Howlett, *J. Phys. Chem. C*, 2016, **120(8)**, 4276-4286, doi: 10.1021/acs.jpcc.5b11746.
[72] T. C. Mendes, X. Zhang, Y. Wu, P. C. Howlett, M. Forsyth and D. R. Macfarlane, *ACS Sustain. Chem. Eng.*, 2019, **7(4)**, 3722-3726, doi: 10.1021/acssuschemeng.8b06212.
[73] A. Ponrouch, D. Monti, A. Boschin, B. Steen, P. Johansson and M. R. Palacín, *J. Mater. Chem. A*, 2015, **3(1)**, 22-42, doi: 10.1039/c4ta04428b.
[74] N. Bucher, S. Hartung, J. B. Franklin, A. M. Wise, L. Y. Lim, H. Y. Chen, J. N. Weker, M. F. Toney and M. Srinivasan, *Chem. Mater.*, 2016, **28(7)**, 2041-2051, doi: 10.1021/acs.chemmater.5b04557.
[75] C. H. Wang, Y. W. Yeh, N. Wongittharom, Y. C. Wang, C. J. Tseng, S. W. Lee, W. S. Chang and J. K. Chang, *J. Power Sources*, 2015, **274**, 1016-1023, doi: 10.1016/j.jpowsour.2014.10.143.
[76] J. P. Parant, R. Olazcuaga, M. Devalette, C. Fouassier and P. Hagenmuller, *J. Solid State Chem.*, 1971, **3(1)**, 1-11, doi: 10.1016/0022-4596(71)90001-6.
[77] D. Monti, A. Ponrouch, M. R. Palacín and P. Johansson, *J. Power Sources*, 2016, **324**, 712-721, doi: 10.1016/j.jpowsour.2016.06.003.
[78] T. A. Unzner and T. Magauer, *Tetrahedron Lett.*, 2015, **56(7)**, 877-883, doi: 10.1016/j.tetlet.2014.12.145.
[79] M. P. Do, N. Bucher, A. Nagasubramanian, I. Markovits, T. Bingbing, P. Fischer, K. P. Loh, F. E. Kühn and M. Srinivasan, *ACS Appl. Mater. Inter.*, 2019, 11, 23972-23981, doi: 10.1021/acsami.9b03279.
[80] K. A. See, K. W. Chapman, L. Zhu, K. M. Wiaderek, O. J. Borkiewicz, C. J. Barile, P. J. Chupas and A. A. Gewirth, *J. Am. Chem. Soc.*, 2016, **138(1)**, 328-337, doi: 10.1021/jacs.5b10987.
[81] O. Tutusaus, R. Mohtadi, T. S. Arthur, F. Mizuno, E. G. Nelson and Y. V. Sevryugina, *Angew. Chem. Int. Edit.*, 2015, **54(27)**, 7900-7904, doi: 10.1002/anie.201412202.
[82] O. Chusid, Y. Gofer, H. Gizbar, Y. Vestfrid, E. Levi, D. Aurbach and I. Riech, *Adv. Mater.*, 2003, **15(7-8)**, 627-630, doi: 10.1002/adma.200304415.
[83] J. Muldoon, C. B. Bucur and T. Gregory, *Chem. Rev.*, 2014, **114(23)**, 11683-11720, doi: 10.1021/cr500049y.
[84] G. A. Elia, K. Marquardt, K. Hoeppner, S. Fantini, R. Lin, E. Knipping, W. Peters, J. F. Drillet, S. Passerini and R. Hahn, *Adv. Mater.*, 2016, **28(35)**, 7564-7579, doi: 10.1002/adma.201601357.
[85] M. Fouletier and M. Armand, *Carbon*, 1979, **17(5)**, 427-429, doi: 10.1016/0008-6223(79)90059-9.
[86] J. V. Rani, V. Kanakaiah, T. Dadmal, M. S. Rao and S. Bhavanarushi, *J. Electrochem. Soc.*, 2013, **160(10)**, A1781-A1784, doi: 10.1149/2.072310jes.
[87] M. C. Lin, M. Gong, B. Lu, Y. Wu, D. Y. Wang, M. Guan, M. Angell, C. Chen, J. Yang, B. J. Hwang and H. Dai, *Nature*, 2015, **520(7547)**, 325-328, doi: 10.1038/nature14340.
[88] Q. Zhao, Y. Lu, Z. Zhu, Z. Tao and J. Chen, *Nano Lett.*, 2015, **15(9)**, 5982-5987, doi: 10.1021/acs.nanolett.5b02116.
[89] M. Yu, W. D. McCulloch, D. R. Beauchamp, Z. Huang, X. Ren and Y. Wu, *J. Am. Chem. Soc.*, 2015, **137(26)**, 8332-8335, doi: 10.1021/jacs.5b03626.
[90] H. Tian, T. Gao, X. Li, X. Wang, C. Luo, X. Fan, C. Yang, L. Suo, Z. Ma, W. Han and C. Wang, *Nat. Commun.*, 2017, **8**, 14083, doi: 10.1038/ncomms14083.
[91] B. Xue, Z. Fu, H. Li, X. Liu, S. Cheng, J. Yao, D. Li, L. Chen and Q. Meng, *J. Am. Chem. Soc.*, 2006, **128(27)**, 8720-8721, doi: 10.1021/ja057791v.
[92] T. C. Mendes, C. Xiao, F. Zhou, H. Li, G. P. Knowles, M.

Hilder, A. Somers, P. C. Howlett and D. R. MacFarlane, *ACS Appl. Mater. Inter.*, 2016, **8(51)**, 35243-35252, doi: 10.1021/acsami.6b11716.
[93] T. C. Mendes, F. Zhou, A. J. Barlow, M. Forsyth, P. C. Howlett and D. R. MacFarlane, *Sustainable Energy Fuels*, 2018, **2(4)**, 763-771, doi: 10.1039/c7se00547d.
[94] T. Mao, S. Wang, X. Wang, F. Liu, J. Li, H. Chen, D. Wang, G. Liu, J. Xu and Z. Wang, *ACS Appl. Mater. Inter.*, 2019, **11(19)**, 17742-17750, doi: 10.1021/acsami.9b00452.
[95] A. A. Chaugule, V. S. Mane, H. A. Bandal, H. Kim and A. S. Kumbhar, *ACS Sustain. Chem. Eng.*, 2019, **7(17)**, 14889-14898, doi: 10.1021/acssuschemeng.9b02997.
[96] B. Xue, H. Wang, Y. Hu, H. Li, Z. Wang, Q. Meng, X. Huang, O. Sato, L. Chen and A. Fujishima, *Photoch. Photobio. Sci.*, 2004, **3(10)**, 918-919, doi: 10.1039/B412647E.
[97] R. Kawano, H. Matsui, C. Matsuyama, A. Sato, M. A. B. H. Susan, N. Tanabe and M. Watanabe, *J. Photoch. Photobio. A*, 2004, **164(1-3)**, 87-92, doi: 10.1016/j.jphotochem.2003.12.019.
[98] Y. Tang, X. Chi, S. Zou and X. Zeng, *Nanoscale*, 2016, **8(10)**, 5771-5779, doi: 10.1039/c5nr07502e.
[99] R. Izumi, Y. Yao, T. Tsuda, T. Torimoto and S. Kuwabata, *J. Mater. Chem. A*, 2018, **6(25)**, 11853-11862, doi: 10.1039/c8ta03465f.
[100] S. Doblinger, J. Lee and D. S. Silvester, *J. Phys. Chemi. C*, 2019, **123(17)**, 10727-10737, doi: 10.1021/acs.jpcc.8b12123.
[101] B. Kumar, M. Asadi, D. Pisasale, S. Sinha-Ray, B. A. Rosen, R. Haasch, J. Abiade, A. L. Yarin and A. Salehi-Khojin, *Nat. Commun.*, 2013, **4**, 2819, doi: 10.1038/ncomms3819.
[102] J. L. DiMeglio and J. Rosenthal, *J. Am. Chem. Soc.*, 2013, 1**35(24)**, 8798-8801, doi: 10.1021/ja4033549.
[103] J. Shen, R. Kortlever, R. Kas, Y. Y. Birdja, O. Diaz-Morales, Y. Kwon, I. Ledezma-Yanez, K. J. Schouten, G. Mul and M. T. Koper, *Nat. Commun.*, 2015, **6**, 8177, doi: 10.1038/ncomms9177.
[104] K. P. Kuhl, T. Hatsukade, E. R. Cave, D. N. Abram, J. Kibsgaard and T. F. Jaramillo, *J. Am. Chem. Soc.*, 2014, **136(40)**, 14107-14113, doi: 10.1021/ja505791r.
[105] X. Kang, Q. Zhu, X. Sun, J. Hu, J. Zhang, Z. Liu and B. Han, *Chem. Sci.*, 2016, **7(1)**, 266-273, doi: 10.1039/c5sc03291a.
[106] K. Manthiram, B. J. Beberwyck and A. P. Alivisatos, *J. Am. Chem. Soc.*, 2014, **136(38)**, 13319-13325, doi: 10.1021/ja5065284.
[107] F. S. Roberts, K. P. Kuhl and A. Nilsson, *Angew. Chem. Int. Edit.*, 2015, **54(17)**, 5179-5182, doi: 10.1002/anie.201412214.
[108] Y. Liu, S. Chen, X. Quan and H. Yu, *J. Am. Chem. Soc.*, 2015, **137(36)**, 11631-11636, doi: 10.1021/jacs.5b02975.
[109] Q. Lu, J. Rosen, Y. Zhou, G. S. Hutchings, Y. C. Kimmel, J. G. Chen and F. Jiao, *Nat. Commun.*, 2014, **5**, 3242, doi: 10.1038/ncomms4242.
[110] D. Yuan, C. Yan, B. Lu, H. Wang, C. Zhong and Q. Cai, *Electrochim. Acta*, 2009, **54(10)**, 2912-2915, doi: 10.1016/j.electacta.2008.11.006.
[111] L. Zhang, D. Niu, K. Zhang, G. Zhang, Y. Luo and J. Lu, *Green Chem.*, 2008, **10(2)**, 202-206, doi: 10.1039/b711981j.
[112] H. Yang, Y. Gu, Y. Deng and F. Shi, *Chem. Commun.*, 2002, **2(3)**, 274-275, doi: 10.1039/b108451h.
[113] Q. Zhu, J. Ma, X. Kang, X. Sun, H. Liu, J. Hu, Z. Liu and B. Han, *Angew. Chem. Int. Edit.*, 2016, **55(31)**, 9012-9016, doi: 10.1002/anie.201601974.
[114] N. Hollingsworth, S. F. Taylor, M. T. Galante, J. Jacquemin, C. Longo, K. B. Holt, N. H. De Leeuw and C. Hardacre, *Angew. Chem. Int. Edit.*, 2015, **54(47)**, 14164-14168, doi: 10.1002/anie.201507629.
[115] C. Yan, B. Lu, X. Wang, J. Zhao and Q. Cai, *J. Chem. Technol. Biot.*, 2011, **86(11)**, 1413-1417, doi: 10.1002/jctb.2647.
[116] S. Seki, N. Serizawa, S. Ono, K. Takei, K. Hayamizu, S. Tsuzuki and Y. Umebayashi, *J. Chem. Eng. Data*, 2019, **64(2)**, 433-441, doi: 10.1021/acs.jced.8b00334.
[117] N. Arai, H. Watanabe, T. Yamaguchi, S. Seki, K. Ueno, K. Dokko, M. Watanabe, Y. Kameda, R. Buchner and Y. Umebayashi, *J. Phys. Chem. C*, 2019, **123**, 30228-30233, doi: 10.1021/acs.jpcc.9b10770.
[118] D. Bedrov, J. P. Piquemal, O. Borodin, A. D. MacKerell Jr, B. Roux and C. Schröder, *Chem. Rev.*, 2019, **119(13)**, 7940-7995, doi: 10.1021/acs.chemrev.8b00763.
[119] H. Watanabe, T. Umecky, N. Arai, A. Nazet, T. Takamuku, K. R. Harris, Y. Kameda, R. Buchner and Y. Umebayashi, *J. Phys. Chem. B*, 2019, **123(29)**, 6244-6252, doi: 10.1021/acs.jpcb.9b03185.
[120] H. Zhu, S. Zhu, Z. Jia, S. Parvinian, Y. Li, O. Vaaland, L. Hu and T. Li, *P. Natl. Acad. Sci. USA*, 2015, **112(29)**, 8971-8976, doi: 10.1073/pnas.1502870112.
[121] K. Rohrbach, Y. Li, H. Zhu, Z. Liu, J. Dai, J. Andreasen and L. Hu, *Chem. Commun.*, 2014, **50(87)**, 13296-13299, doi: 10.1039/c4cc04817b.
[122] Z. Gui, H. Zhu, E. Gillette, X. Han, G. W. Rubloff, L. Hu and S. B. Lee, *ACS Nano*, 2013, **7(7)**, 6037-6046, doi: 10.1021/nn401818t.
[123] S. Wang, F. Jiang, X. Xu, Y. Kuang, K. Fu, E. Hitz and L. Hu, *Adv. Mater.*, 2017, **29(35)**, 1702498, doi: 10.1002/adma.201702498.
[124] S. Wang, T. Li, C. Chen, W. Kong, S. Zhu, J. Dai, A. J. Diaz, E. Hitz, S. D. Solares, T. Li and L. Hu, *Adv. Funct. Mater.*, 2018, **28(24)**, 1707491, doi: 10.1002/adfm.201707491.
[125] H. Xie, C. Yang, K. Fu, Y. Yao, F. Jiang, E. Hitz, B. Liu, S. Wang and L. Hu, *Adv. Energy Mater.*, 2018, **8(18)**, 1703474, doi: 10.1002/aenm.201703474.
[126] T. Li, X. Zhang, S. D. Lacey, R. Mi, X. Zhao, F. Jiang, J. Song, Z. Liu, G. Chen, J. Dai, Y. Yao, S. Das, R. Yang, R. M. Briber and L. Hu, *Nat. Mater.*, 2019, **18(6)**, 608-613, doi: 10.1038/s41563-019-0315-6.
[127] Hu and S. B. Lee, *ACS Nano*, 2013, **7(7)**, 6037-6046, doi: 10.1021/nn401818t.
[128] S. Wang, F. Jiang, X. Xu, Y. Kuang, K. Fu, E. Hitz and L. Hu, *Adv. Mater.*, 2017, **29(35)**, 1702498, doi:

10.1002/adma.201702498.
[129] S. Wang, T. Li, C. Chen, W. Kong, S. Zhu, J. Dai, A. J. Diaz, E. Hitz, S. D. Solares, T. Li and L. Hu, *Adv. Funct. Mater.*, 2018, **28(24)**, 1707491, doi: 10.1002/adfm.201707491.
[130] H. Xie, C. Yang, K. Fu, Y. Yao, F. Jiang, E. Hitz, B. Liu, S. Wang and L. Hu, *Adv. Energy Mater.*, 2018, **8(18)**, 1703474, doi: 10.1002/aenm.201703474.
[131] T. Li, X. Zhang, S. D. Lacey, R. Mi, X. Zhao, F. Jiang, J. Song, Z. Liu, G. Chen, J. Dai, Y. Yao, S. Das, R. Yang, R. M. Briber and L. Hu, *Nat. Mater.*, 2019, **18(6)**, 608-613, doi: 10.1038/s41563-019-0315-6.

Publisher's Note

